HYDROLOGICAL PROCESSES, VOL. 9, 161–182 (1995)

THE $\ln(a/\tan\beta)$ INDEX: HOW TO CALCULATE IT AND HOW TO USE IT WITHIN THE TOPMODEL FRAMEWORK

P. F. QUINN, K. J. BEVEN AND R. LAMB

Centre for Research in Environmental Systems and Statistics, Lancaster University, Lancaster LA1 4YQ, UK

ABSTRACT

Topographic indices may be used to attempt to approximate the likely distribution of variable source areas within a catchment. One such index has been applied widely using the distribution function catchment model, TOPMODEL, of Beven and Kirkby (1979). Validation of the spatial predictions of TOPMODEL may be affected by the algorithm used to calculate the model's topographic index. A number of digital terrain analysis (DTA) methods are therefore described for use in calculating the TOPMODEL topographic index, $\ln(a/\tan\beta)$ (a = upslope contributing area per unit contour; $\tan\beta$ = local slope angle). The spatial pattern and statistical distribution of the index is shown to be substantially different for different calculation procedures and differing pixel resolutions. It is shown that an interaction between hillslope contributing area accumulation and the analytical definition of the channel network has a major influence on calculated $\ln(a/\tan\beta)$ index patterns. A number of DTA tests were performed to explore this interaction. The tests suggested that an 'optimum' channel initiation threshold (CIT) may be identified for positioning river headwaters in a raster digital terrain model (DTM). This threshold was found to be dependent on DTM grid resolution. Grid resolution is also suggested to have implications for the validation of spatial model predictions, implying that 'optimum' TOPMODEL parameter sets may be unique to the grid scale used in their derivation. Combining existing DTA procedures with an identified CIT, a procedure is described to vary the directional diffusion of contributing area accumulation with distance from the channel network.

KEY WORDS TOPMODEL digital terrain analysis; soil moisture; spatial and temporal model predictions

INTRODUCTION

This paper is directed at scientists and engineers who wish to use topographic indices for the functional representation of catchment hydrological processes that may be related to geomorphic form. The paper may also be of interest to those who have already used hydrological models and topographic indices. Current methods are discussed for calculating topographic index distributions using digital terrain analysis (DTA). Also discussed are issues concerning the spatial resolution of the DTA methods used to calculate the topographic index used in the catchment model TOPMODEL (Beven and Kirkby, 1979).

With the evolution of affordable, powerful computers and the availability of digital terrain models (DTMs), DTA has become a useful tool with many applications (Beven and Moore, 1993). There is now also a considerable interest in computer models of catchment hydrology, and there is a wide range of model structures with differing aims (Bowles and O'Connell, 1991). Two models which involve the use of topographic indices are TOPMODEL and a similar model, TAPES (O'Loughlin 1981; 1986; Moore *et al.*, 1986). TOPMODEL has been applied to the modelling of soil moisture fluxes, geochemical fluxes, evapotranspiration, erosion and sedimentation. Examples of TOPMODEL applications in a range of locations may be found in the following papers: Beven *et al.* (1984); Hornberger *et al.* (1985); Beven (1986); Wood *et al.* (1988); Famiglietti and Wood (1991); Robson *et al.* (1992); and Quinn and Beven (1993). Of particular interest in this paper is the relationship between a model that uses a topographic index and the DTA methods used to calculate the pattern of that index.

CCC 0885–6087/95/020161–22

Received 8 February 1994
Accepted 12 April 1994

Digital terrain analysis in hydrology was concentrated initially on direct morphometry, for instance the estimation of catchment size, boundary positions and river delineation (Band, 1986; Morris and Herdeegen, 1988; Tarboton *et al.*, 1991). This type of analysis followed from the earlier development of deterministic hydrological models that were based on morphometric parameters such as area ratios and stream density (Strahler, 1957). An example of such a model is the geomorphological instantaneous unit hydrograph of Rodriguez-Iturbe and Valdes (1979). A different modelling approach has emerged informed by research into the dynamics of variable source areas (Hewlett and Hibbert, 1963; Dunne and Black, 1970; Sklash and Farvolden, 1979). The significance of catchment topography in controlling the spatial pattern of storm-flow source areas was recognized by Hewlett and Troendle (1975), who suggested a relationship between slope contours and the likely distribution of source areas. Subsequently, TOPMODEL was developed, based on a group of concepts which may be construed as an interface between basin topography and flow patterns in time and space. TOPMODEL utilizes a topographic index which represents a theoretical estimation of the accumulation of flow at any point. The distribution of the index may be calculated for any catchment and is used as a basis for the prediction of source areas, saturation excess overland flow and subsurface flows. The index has the form

$$\ln(a/\tan\beta)$$

where, in terms of a raster DTM, a = the upslope area, per unit contour length, contributing flow to a pixel; $\tan\beta$ = the local slope angle acting on a cell (this is taken to approximate the local hydraulic gradient under steady-state conditions).

An alternative expression is the combined soils/topographic index

$$\ln(a/T_0\tan\beta)$$

where T_0 = the lateral transmissivity of the soil profile when the water-table just intersects the surface. The logarithmic form arises from an assumption that the transmissivity of the soil falls off with depth (Beven, 1986).

In early applications of TOPMODEL, the $\ln(a/\tan\beta)$ index was calculated manually using contour data. However, the advent of gridded DTMs has allowed this procedure to be automated. The first such automated procedure was reported by Quinn *et al.* (1991) (although the program had already been in existence for some time). This form of DTA makes it convenient to calculate the distributed topographic index for any catchment, given a suitable DTM. It is therefore unsurprising that the topographic index $\ln(a/\tan\beta)$ has often been used to visualize macroscale flow patterns within catchments.

However, use of the $\ln(a/\tan\beta)$ index in TOPMODEL applications has led to some debate over the interaction between model assumptions and DTA methods. Two immediate issues are to be addressed in this paper, namely the appropriate DTM resolution for modelling exercises and the treatment of rivers in the calculation of the $\ln(a/\tan\beta)$ index. We have always believed that both TOPMODEL and the methods used to calculate $\ln(a/\tan\beta)$ index should be open to development — this is why DTA routines have never been integrated with the procedural TOPMODEL as a single software package. The introduction of new field data and the experience of differing model demands serve to stimulate the development of new modelling ideas. It is almost inevitable that some modification to the model structure may be suggested by each different application of TOPMODEL. Hence it has been expedient to keep separate the procedures used to implement TOPMODEL from the DTA routines used to calculate the $\ln(a/\tan\beta)$ index. However, it is felt that the development of DTA procedures should not be overlooked.

This paper will discuss only gridded forms of DTMs and DTA. The most common DTM format is the regular grid, and the most common grid sizes encountered are between 10 and 50 m (the UK national database uses a 50 m grid and the US national database is at a 30 m resolution). The DTM creation procedure is still the most difficult step in the topographic analysis, but here it is assumed that any problems have been resolved before proceeding to the calculation of the $\ln(a/\tan\beta)$ index. It is also assumed that 'sinks' (i.e. grid cells with no outfall) and 'dams' (i.e. interpolation errors in narrow valleys that cause a reservoir of sinks) have been successfully removed.

THE PROBLEMS

A number of questions may be asked of the DTA methods used to calculate the ln(a/tanβ) index. The following questions have been prompted by users of TOPMODEL:

1. What effect does DTM grid size have on the calculation of the ln(a/tanβ) index?
2. How should accumulated contributing area be shared out in space? What controls the apportioning of accumulated area between pixels/grid cells?
3. How should permanent and ephemeral channels interact with the accumulation of contributing area, and how can this interaction be accounted for using DTA procedures?

TOPMODEL has been applied using DTMs with grid sizes ranging between 1 and 50 m. Grid sizes of around 100 m are considered to be too large for the application of the ln(a/tanβ) index, which requires a finer grid resolution to depict the topographical form of individual hillslopes. Grid size has a direct effect on the calculation of accumulated contributing area in the ln(a/tanβ) index. Accumulated area may be shared out differently over space according to grid size. The spatial distribution of the accumulated area term of ln(a/tanβ) effectively represents the partitioning of hypothetical downslope flows. This partitioning is a primary influence on the eventual pattern of the index for any basin. The DTA methods currently used with TOPMODEL have seemingly arbitrary rules for apportioning flow in space. Although hydrographs may be predicted with some success even if the calculation of the topographic index changes, the internal validation of spatially distributed model variables relies on the pattern of the ln(a/tanβ) index being correctly calculated. Internal validation of model processes is desirable, but is still qualitative for TOPMODEL. This may reflect, in part, the fact that there is no 'correct' way of apportioning accumulated area in the DTA calculations.

We suggest here that flow partitioning in space by DTA is still very much an open subject. Several methods of apportioning accumulated area will be discussed below.

The positioning of river cells in the catchment DTM is important to the eventual pattern of the ln(a/tanβ) index. It is shown later how considerable bias may be introduced to the spatial pattern of the index, should the hydrological role of cells or pixels containing a river channel not be taken into account.

Perhaps the two main aims of the catchment modeller are: (1) the prediction of hydrographs; and (2) the determination of the processes producing flow in the catchment and their spatial distributions. This may allow the internal state validation of the model, something perceived by many hydrologists to be the next major modelling goal.

Model validation against distributed internal state measurements leads to a fundamental problem in that predicted and observed data may well be scale dependent (Beven, 1987; 1989). The modeller works with a mixture of areally integrated catchment data (e.g. rain, flow and evaporation) and internal state measurements, generally sampled at points (e.g. piezometers, gravimetric samples, TDR probes and capacitance probes). Does it follow that model DTM scales should be reduced to approach the point scale if internal state predictions are to be made? Gridded remote sensing data, or geographical information system (GIS) data, such as vegetation indices, may be available. These data potentially allow distributed predictions to be compared with observed patterns held at the same scale, but may themselves be subject to sampling or interpolation errors.

CURRENT TOPMODEL THEORY

TOPMODEL will not be discussed here at great length. Full details are given by Beven (1986) and Quinn and Beven (1993). TOPMODEL can be used to predict both hydrographs and a distributed water-table. The TOPMODEL predicted hydrograph consists of a subsurface, lumped saturated zone response and saturation–excess runoff generated from dynamic source areas. Water-table depths may be predicted for any catchment DTM pixel. Modification of the local water-table depth by capillary fringe effects, by evapotranspiration through a root zone and by recharge through an unsaturated zone store gives an estimate of local soil moisture status. Calculated local water-table depths depend on the value of the ln(a/tanβ) index at a point.

TOPMODEL works through the use of simple distribution empirical functions. The distribution function relating the $\ln(a/\tan\beta)$ index to fractional areas of the catchment is of primary concern in this paper. When expressed as a combined soils/topographic index, the transmissivity parameter T_0 is commonly taken to be a constant, lumped catchment parameter. This has a simple scaling effect on the topographic distribution function. Should spatial soil data be available, or an obvious pattern in catchment soil characteristics exist, then a spatially distributed T_0 may be used and included in the DTA procedures for calculating $\ln(a/\tan\beta)$. In this paper, however, it will be assumed that T_0 is constant in space. The main concern here is thus the effect of topography alone on patterns of likely water accumulation in the catchment.

Figure 1A shows a catchment DTM and Figure 1B the resultant map of the calculated $\ln(a/\tan\beta)$ index. By analysing the range and areal extent of $\ln(a/\tan\beta)$ values, a single distribution function can be derived (Figure 1C). Pixels having the same value of $\ln(a/\tan\beta)$, or having a $\ln(a/\tan\beta)$ value within a specified range, are assumed to behave in a hydrologically similar manner. These pixels may therefore be modelled simultaneously, hence reducing the number of calculations performed by the model. Predictions of local water-table depth may be made for each value, or increment, of the topographic index distribution function and the predictions mapped back into space according to the pattern of the $\ln(a/\tan\beta)$ index. Predicted water-table patterns will thus follow the outline of the $\ln(a/\tan\beta)$ index map, with predicted saturated source area expanding and contracting as the water balance of the model changes.

Figure 2 shows the nature of the time transformation embodied with TOPMODEL. It is assumed, for simplicity, that the recession response function of the catchment is constant (Figure 2A). Hence, a unique 'master recession curve' (Nathan and McMahon 1990) may be constructed for any catchment by analysing recession curves covering a range of flow-rates. Following TOPMODEL assumptions of a lumped saturated

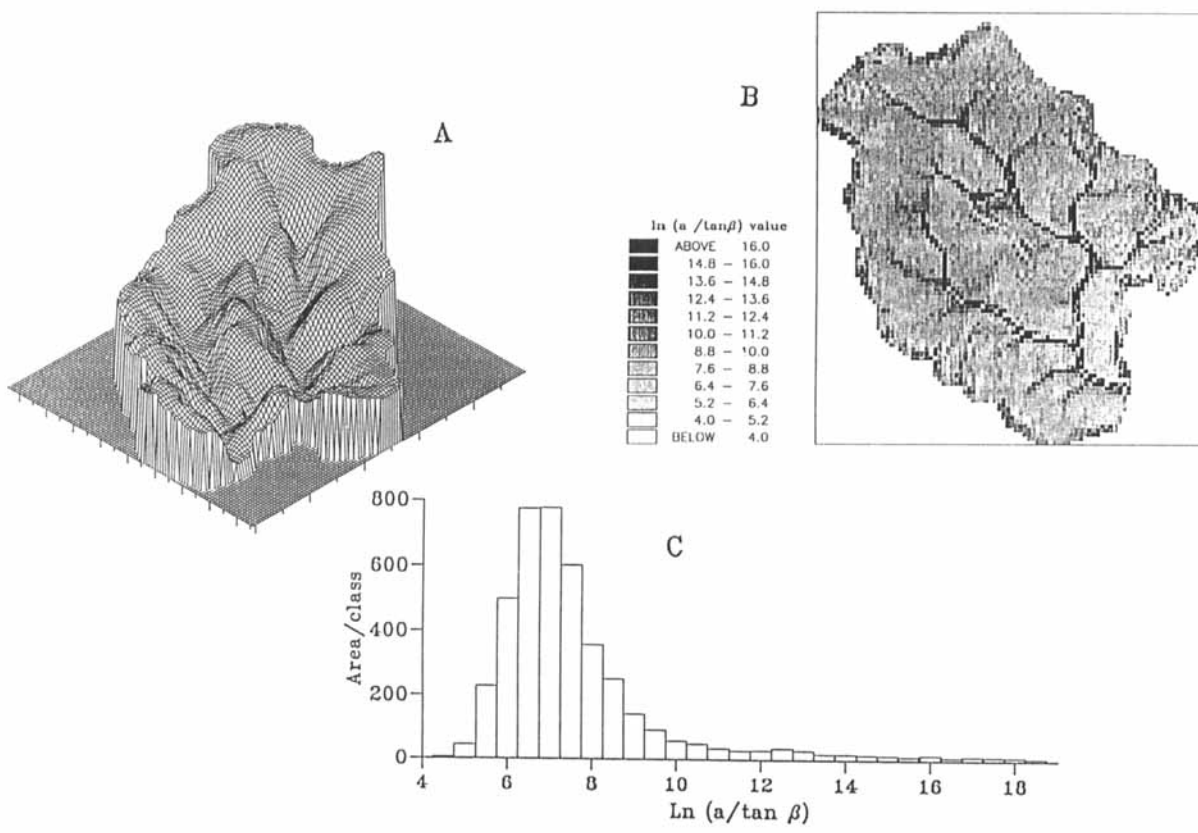

Figure 1. Spatial conceptualization of TOPMODEL. (A) 50 m grid cell DTM for the River Wye at Plynlimon. (B) $\ln(a/\tan\beta)$ pattern for the DTM in (A). (C) Areal distribution function for (B) that will be used by TOPMODEL

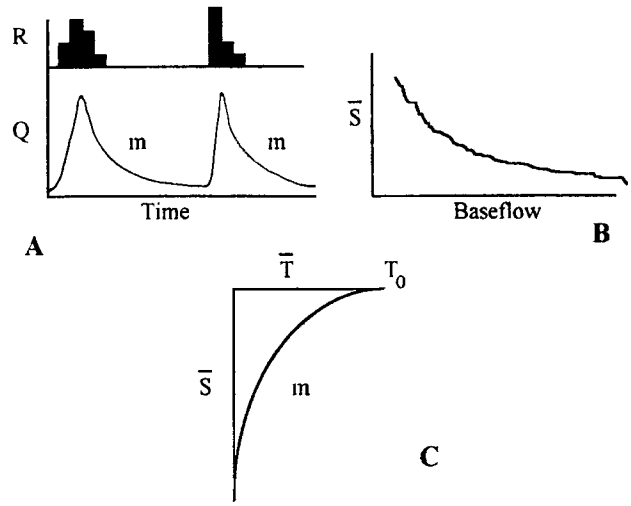

Figure 2. Temporal conceptualization of TOPMODEL. (A) Typical rainfall–runoff relationship where R is the rainfall intensity, Q is the discharge and m is the rate of change of the recession curve. (B) Relationship between the baseflow discharge and the average soil moisture deficit ($\bar{S}$) of the catchment. (C) Relationship of transmissivity with ($\bar{S}$) where $\bar{T}$ is the average operating transmissivity and T_0 is the transmissivity when saturated

zone store, the master recession curve may be taken to represent the relationship between saturated zone output (notionally 'baseflow') and time. From this relationship may be calculated a function relating saturated zone storage (or storage deficit) to baseflow (Figure 2B). This saturated zone baseflow response has been approximated by an exponential function of storage (Beven and Kirkby, 1979). Similarly, the decline of local transmissivity with decreasing storage in the soil profile has been approximated by an exponential function

$$T_i = T_0 \exp(-S_i/m)$$

where T_i = the current transmissivity of the catchment; S_i = current local saturated zone storage deficit; and m is a parameter controlling the shape of the function.

By accounting continuously for the total soil moisture deficit in the catchment, local saturated zone deficits can be calculated using an equation derived by Beven (1986)

$$S_i = \bar{S} + m(\gamma - \ln(a/T_0 \tan\beta)$$

where

$$\gamma = \frac{1}{np}\sum \ln(aT_0 \tan\beta_i)$$

is the catchment average of the soils/topographic index and np is the total number of pixels.

EXISTING METHODS FOR CALCULATING THE ln(a/tanβ) INDEX

In an attempt to represent the convergence or divergence of flow under the control of topographic curvature, Quinn *et al.* (1991) developed a multiple flow direction algorithm to calculate accumulated contributing areas across adjacent pixels. This routine was written initially to work on 50 m resolution DTMs. The routine is effectively a form of subgrid interpolation which shares contributing area in accordance with the shape of the contours passing through a given grid cell relative to those of its neighbours.

Figure 3 shows the original multiple direction flow sharing algorithm for an example DTM with a 50 m grid resolution. The main variables in the slope algorithm are the angle between the adjacent pixels, the postulated contour length depending on flow direction (0·5 weighting for cardinal directions and 0·35

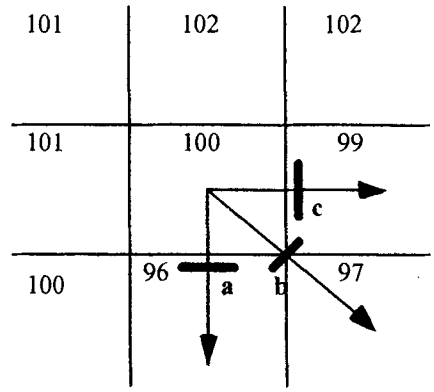

a = 0.5* tan ((100-96)/dx1) = 65.55%
b = 0.35 * tan ((100-97)/dx2) = 23.01%
c = 0.5 * tan ((100-99)/dx1) =15.44%

Figure 3. Existing multiple flow direction apportioning algorithm (Quinn *et al.*, 1991)

for a diagonal weighting) and the flow lengths *dx1* and *dx2*. Length *dx1* is set to 50 m and *dx2* to 70·1 m to account for the longer flow path between downslope diagonal pixels. When summed across a series of downslope cells it is in contact with, the algorithm produces a series of weighted flow proportions. The current accumulated area in each cell is then passed to its neighbours using these calculated proportions.

The single flow direction algorithm (O'Callaghan and Mark, 1984) does not require a contour length term as every pixel has the same contour length. However, multiple flow direction algorithms have variable outflow directions that are dependent on a cell's neighbours, hence the contour length must be taken into consideration. Figure 4 has been produced to show how the contour length effects the local index value. For two identical upslope areas, the calculated value of *a* can be very different. For pixel analysis the increased number of outflow directions has the effect of lengthening the contour length and, hence, must be considered.

TESTING DTA PROCEDURES

The DTM and contour information used here were derived from the 1 : 10 000 Hunting survey maps for the Plynlimon area of mid-Wales as produced for the Institute of Hydrology. The first DTM, Figure 5, is a subarea of Figure 1. The area has been chosen to contain enough cells to show the pattern of the index (for 50 m grid cells), but not so many as to cause the results to become hidden. A headwater catchment of Figure 5 was then digitized using a 1 : 10 000 contour map and a series of new DTMs were produced by simple bi-linear interpolation using the UNIRAS suite of programs. The pixel sizes chosen for the new DTMs were 5, 10, 25 and 50 m, and can be seen in Figures 6A, B, C and D, respectively.

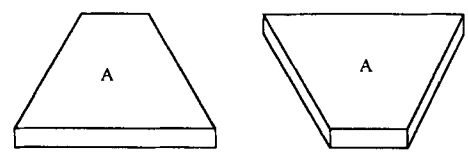

a1 = A/cld1 a2 = A/cld2
cld = contour length

Figure 4. Effect of varying contour length (*cld*) on the index value despite both situations having the same upslope area (*A*)

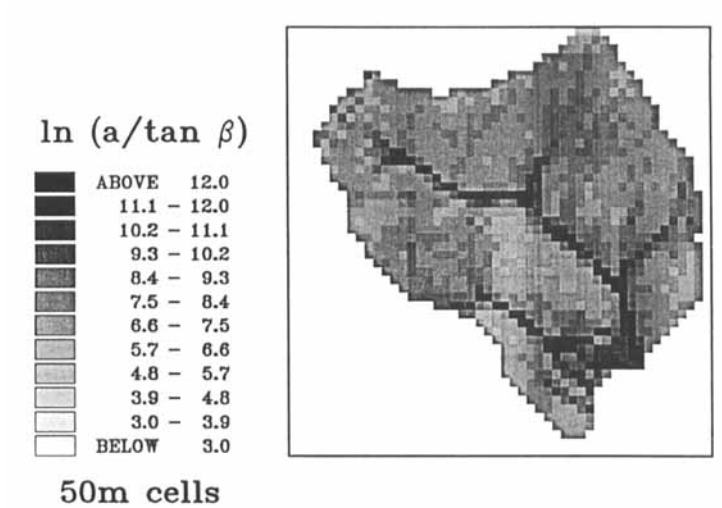

Figure 5. Subsection of Figure 1B showing the ln(a/tanβ) pattern for the 50 m control DTM data set

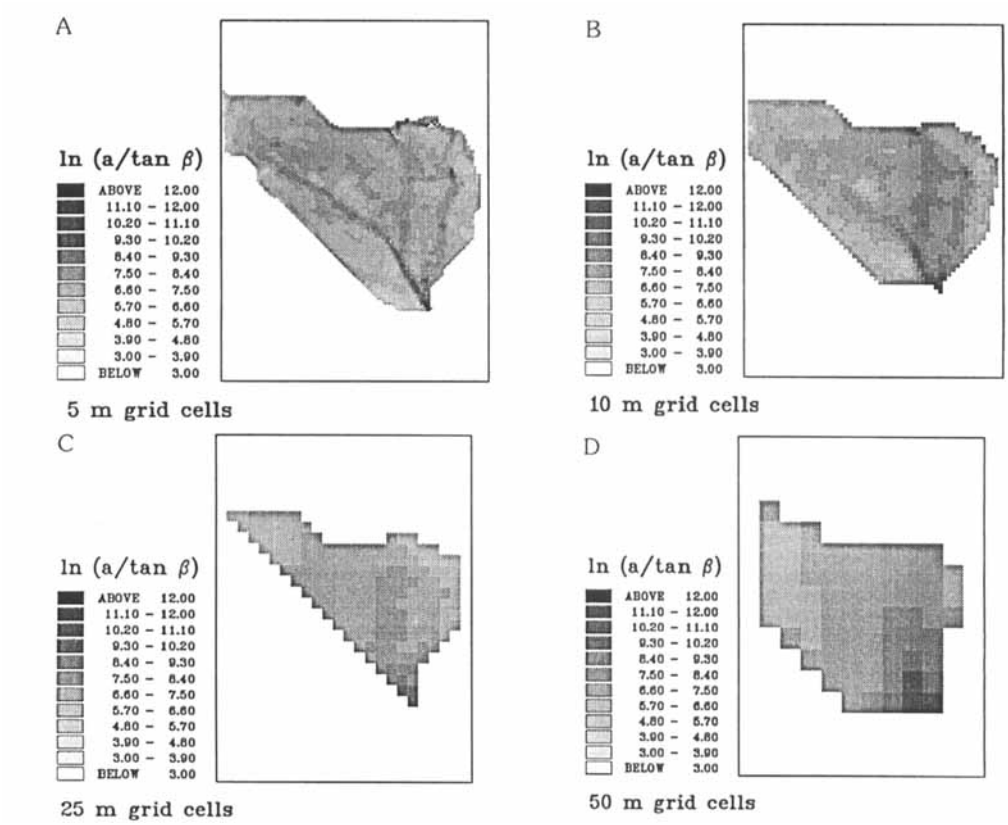

Figure 6. Subcatchment of Figure 5 showing the same area interpolated onto different DTM grid sizes and the subsequent ln(a/tanβ) patterns. (A) 5 m; (B) 10 m; (C) 25 m; and (D) 50 m

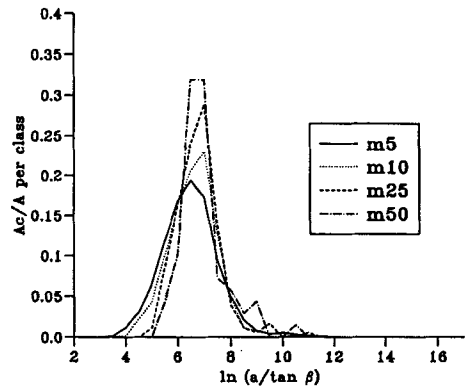

Figure 7. Effect of changing grid size on the distribution function based on the patterns of Figure 6

DIGITAL TERRAIN ANALYSIS: THE PROBLEMS

Grid size

The first problem of grid size is clear when analysing Figures 5 and 6. Although the pattern of Figures 1 and 5 are intuitively reasonable (due to the relatively large number of cells), a detailed study of the Figure 5 pattern compared with Figure 6D shows the problem of areal averaging and the deterioration of resolution. Figure 6A shows a similar pattern to the 50 m resolution of Figure 5 — that is, it is intuitively correct — but Figure 6A and 6D are completely different. The fact that a pattern looks intuitively correct can be misleading, especially when compared with a fine grid scale equivalent. However, the 50 m resolution, although unable to mimic local flux, may well be a good representation of the macroscale flux of the hillslope soil moisture in terms of reflecting gross hillslope convergence and divergence. The 50 m DTM of this small catchment only reflects the build-up of flow downslope and thus exhibits a gradient towards a higher order stream and will tend to ignore the existence of the lower order channels. Small channels are 'hidden' within the large-scale grid cell.

The second problem is that a loss in resolution gives a similar loss of boundary information, hence it becomes difficult to even define accurate catchment boundaries (as can be seen with the 25 and 50 m DTMs).

If point field data were collected for this headwater it would tend to exhibit a pattern of behaviour akin to the 5 m DTM (Figure 6A) and not the 50 m DTM. Hence a first conclusion would be that 50 m DTMs cannot be used to predict point data values. Conversely, point field measurements would have to be

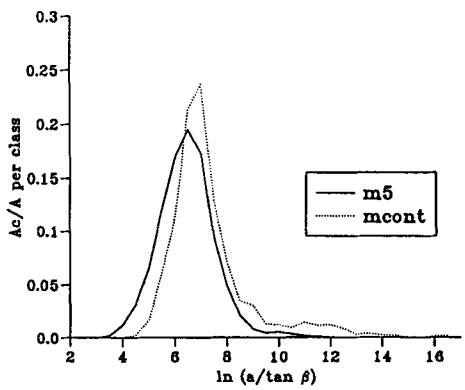

Figure 8. Comparison of the 5 m $\ln(a/\tan\beta)$ distribution of Figure 6A and that of the control DTM of Figure 5, where *mcont* is the 50 m control DTM

lumped together carefully to validate the prediction of a 50 m DTM. This lumping procedure may itself be prone to error, given the local heterogeneity of the soil characteristics.

The third problem is, how does a change in grid size affect the lumped distribution function that is used within TOPMODEL? Figures 7 and 8 have been produced for analysis. Figure 7 shows the distribution functions for Figure 6. Although a distribution function has been produced for Figures 6C and 6D (25 and 50 m, respectively), they do not contain many pixels, which has an effect on the overall distribution form. For a decrease in pixel size, the centre of the peak is shifted to a lower index value and has a lower peak Ac/A value. Also, there is a much greater percentage of lower ln(a/tanβ) values present. It is obvious that smaller resolution pixels give rise to lower index values, as the plan area of the cell is much reduced. Therefore, for upslope cells the a term is much smaller, but the overall gradient of the cells, (tanβ), tends to be unchanged. It may therefore be concluded that large grid cells exhibit a bias towards larger index values.

Figure 8 shows the 5 m DTM against the control distribution produced for Figure 5. Again, the change in grid size causes a lower distribution peak, which is centred at a lower ln(a/tanβ) value. This is a clearer representation of the relationship between the 5 m and the 50 m grid size. The change in shape and position will affect runoff dynamics in the model. However, these changes will be offset by a change in the parameters m and T_0 when reoptimized. This means that TOPMODEL optimized parameter sets will reflect the grid scale of the particular distribution used in the optimization. This leads to the question of which parameter set is correct. In a functional sense both are valid for flow prediction. However, when tested against internal field data, it may become apparent that finer grid resolution solutions are more appropriate to the observed processes. Both, however, would give a reasonable prediction of hydrographs.

Flow apportioning

There are three options open to DTA to alter the flow apportioning routine: (i) manipulation of the contour length; (ii) forcing flow to move preferentially down steeper flow angles; and (iii) choosing a single flow direction algorithm. This is really a special case of (i) and (ii).

The manipulation of contour length is vital within some algorithms, for example using flow tubes or irregular DTM data (Moore *et al.*, 1986). However, the change that can be effected with a rasterized grid is much less. Chairat and Delleur (1993) showed that the manipulation of the contour length had little effect on the final distribution. The reason is that the contour line distance for a particular grid size has a limited sensible operating range. Figure 9 was produced to show one particular extreme example of contour length adjustment. In this instance no diagonal flow is allowed and only cardinal flow directions are used, i.e. the contour length is the grid size and the diagonal contour length equals zero. Although this affects the number of downhill cells, the length of the summed contours has been increased, hence a similar total contour length value is calculated. As can be seen, the patterns of the distribution function are almost identical.

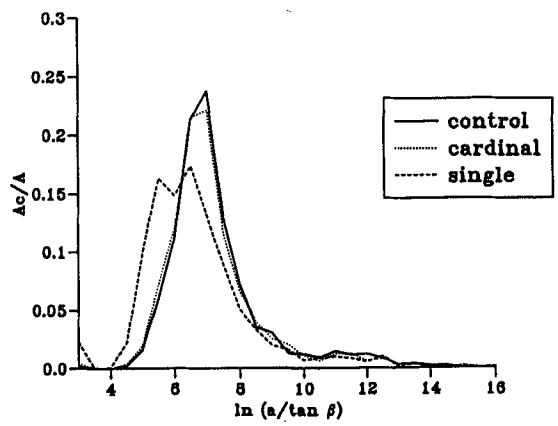

Figure 9. Effect on the distribution function of altering the ln(a/tanβ) contour length algorithm, where *control* is the 50 m *control* DTM, *cardinal* is for the circumstance where *diagonal* flow is suppressed and single is the single flow direction algorithm

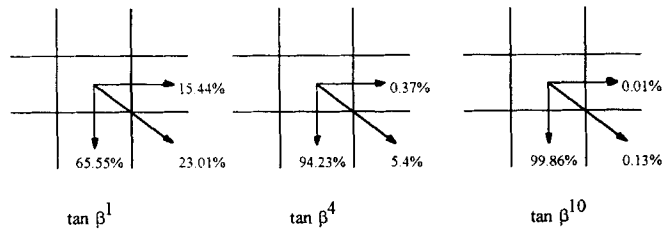

Figure 10. Effect on the flow apportioning routine when raising tanβ to the power h (after Holmgren, in press)

The third flow apportioning option of single flow directions is also shown on Figure 9. As can be seen, this does have a marked effect on the distribution. It could be argued that in some catchments which are extensively rilled, or are perhaps under-drained, such an algorithm may be the most realistic. However, it is widely thought that this method of flow allocation is unrealistic on the hillslope portion of the catchment. Quinn *et al.* (1991) show a number of examples comparing single and multiple flow direction algorithms.

Another method for flow manipulation that is much more powerful is to adjust the amount of water that flows across a particular flow direction dependent on its slope. Holmgren (1994) gives an algorithm where the amount of flow in any one direction is calculated thus

$$d_i = cld(\tan\beta)^h$$

where d_i = the flow proportion in the ith downslope direction and cld = is the same as the original formulation.

Thus $h = 1$ is equivalent to the original multiple flow direction of Quinn *et al.* (1991). Values in excess of 10 tend to give more of a single flow direction approximation. A value of around 100 is equivalent to the single flow direction algorithm. By the simple introduction of this power the pattern can be radically changed. Even if two outflow directions are similar, the effect of a high h power will cause a marked bias towards the steeper angle. This formulation was built into the existing algorithm. Figure 10 shows a worked example that is based on Figure 3. It has been assumed here that the contour length has not changed in size. It could be argued that if the flow was leaving a cell by only one direction, then a reduction in the contour length would occur. However, this would affect the index pattern in the same way as is achieved by increasing the power term only. In fact, if the contour length is allowed to vary inversely with $(\tan\beta)^h$, then the contour length can become infinitesimally small, leading to index values of 100 plus or to computer overflow errors. It is thought that the original contour length algorithm should be the benchmark for analysis and should remain unchanged. The alteration of flow patterns is adequately achieved by using the Holmgren power term.

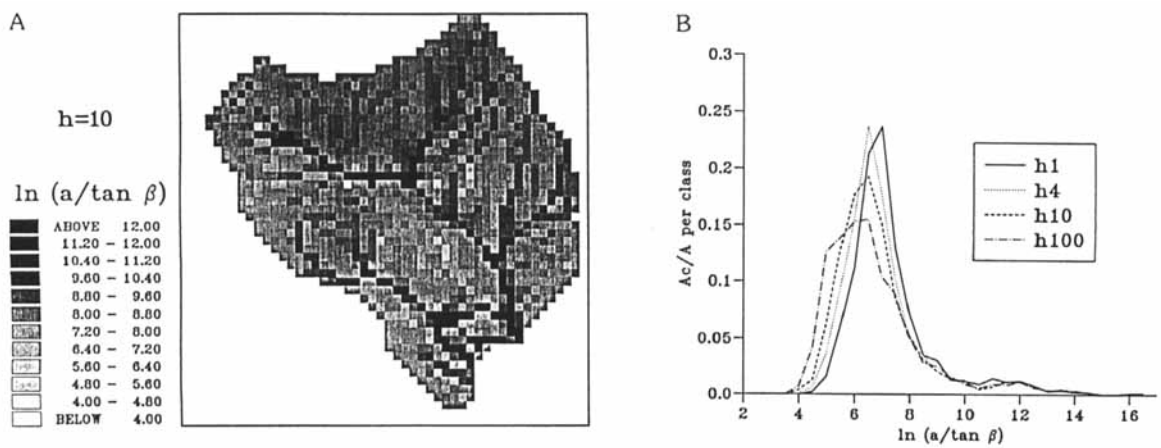

Figure 11. (A) Example map of the ln(a/tanβ) distribution for $h = 10$ for the control DTM. (B) ln(a/tanβ) distribution functions for a range of h values

A similar effect to the Holmgren power was reported by Freeman (1991), where the fraction of flow (f_i) for each individual downslope direction was given by

$$f_i = \frac{S^p}{\Sigma S^p}$$

where S is the calculated slope. Hence p has the same effect as h. In Freeman (1991), p was given the value 1·1, which approximated to a circular contour length shape.

Figure 11 shows the effect of using a power. Figure 11A shows an index pattern that is more akin to a single flow direction algorithm (compared with Figure 5). The effect is that flow is channelled along the steepest line of descent which tends to give an extension of higher index values up the valley bottom and onto the hillslope (which may or may not be desirable). This causes a reduction in the available upslope area flowing into many of the other hillslope cells, causing a reduction in the index values for these cells. This can be seen in Figure 11B, where $h = 1$ is the original and $h = 100$ is the single flow direction approximation. It can be seen that at the upper tail-end of the distribution the 'channel cells' are unchanged, but the 'hillslope cells' are forced to lower values.

This analysis was repeated on the 5 m headwater DTM. It can be seen in Figure 12A that $h = 10$ has not had a drastic effect on the overall pattern (compared with Figure 6A). A value of $h = 50$ (Figure 12B) gives the typical single flow direction pattern. This suggests that for larger pixels the effect of flow straightening is more striking due to the reallocation of the larger plan surface area. Again, it is suggested that an optimum solution based on a test against field evidence will probably depend on the grid size chosen. For example, with a 50 m grid if a value of $h = 10$ is used, it may be necessary to use a value of $h = 50$ with a 5 m grid to produce the same final pattern as based on field evidence.

Interaction of the channel with flow accumulation

The pattern produced by the original algorithm has always shown a strong riparian area and a clear valley bottom structure. The routine is very sensitive to the break in slope at the lower hillslope on to the valley bottom. It is an intuitively appealing pattern and is one reason for the popularity of the index. However, some of the assumptions of flow accumulation can come into question as regards flow build up: (1) what happens to flow when it reaches a channel — does it enter the channel and stay there? and (2) should flow accumulation be allowed downslope to the catchment outfall despite the presence of a channel feature?

Two flow phenomena occur that are caused by the lack of a channel feature in the multiple flow direction algorithm. When flow reaches the valley bottom the flow will braid back and forth across the flatter area, as

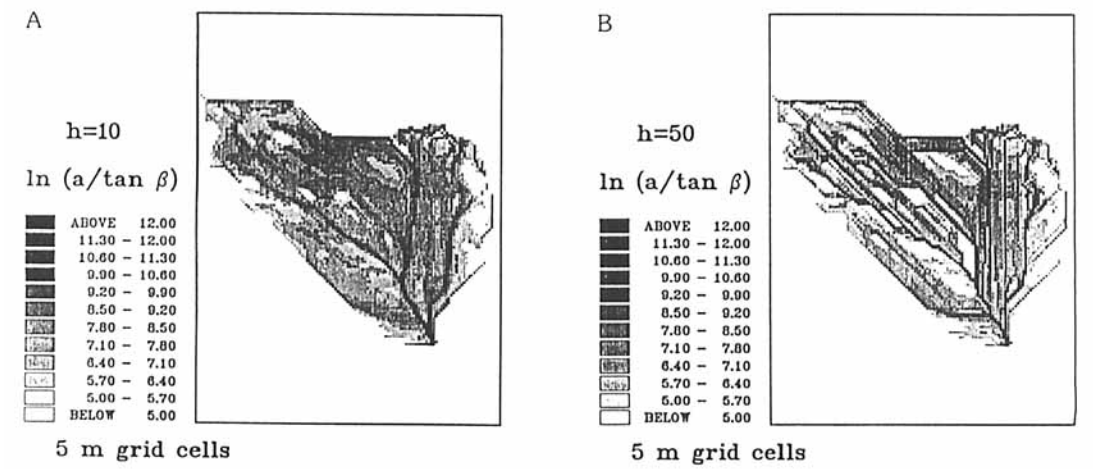

Figure 12. Changing the h parameter on the 5 m DTM of Figure 6A. (A) $h = 10$ and (B) $h = 50$ (similar to the single flow direction algorithm)

controlled by the major break inslope onto the valley bottom. Hence there is generally a set of higher values in the valley bottom due to flow braiding. This is not necessarily an unrealistic effect, and the flow phenomena may be maintained if desired.

The second problem can be clearly seen in Figure 13, a map of the accumulated upslope area for each pixel for the DTM seen in Figure 1A. If flow is allowed to continuously build up downstream, then there will be a large value in the a term in 'channel' cells closer to the outfall. The total upslope area at the outfall is $10{\cdot}5\,km^2$, thus giving a large index value. Again, this may be a desirable phenomena to some field hydrologists. It can also be seen at certain points along the valley bottom that the area value occasionally decreases before increasing again. This is a direct effect of the flow braiding mentioned above. It is possible that flow, when reaching a channel, will tend to flow into that channel and remain there, until exported from the catchment. This is especially true of upland catchments such as the case shown here. The 50 m grid cells represent $2500\,m^2$ of plan surface and the channel feature is only a few metres wide. The channel is thus in reality a subgrid scale feature that contains the upslope accumulated area. The surrounding hillslope portion will have its own upslope area. If the DTA algorithm is left unaltered, the index values lying along the river and especially at the outfall will remain semi-permanent source areas for runoff. In essence it can be implied that the channel and riparian area is $2500\,m^2$ in size for 50 m cells. For this reason, an algorithm has been introduced that flags cells containing a channel for special attention. If the pixel size is sufficiently small or the channel feature sufficiently large then this special routine may not be required and the whole cell should be flagged as a river cell (again the pixel would need a special flag). Even for the case of the 5 m DTM of Figure 6A, channels cells have to be flagged as the channel surface area is still small compared with the plan area of $25\,m^2$. This topic of channel hillslope interaction is important as major variable source areas are found in and around channels and channel heads.

It is possible to use the cumulative area as a threshold for river endings (Morris and Heerdegan, 1989) and this procedure is chosen here. Using the flow accumulation algorithms for calculating $\ln(a/\tan\beta)$ a test can be made to see if some channel initiation threshold (CIT) has been crossed. The CIT is an assumed value of upslope area beyond which a permanent channel will be specified. Therefore, if the CIT is crossed a cell is flagged for special attention. Subsequent downstream cells are thus labelled as 'cells containing a channel', as it is assumed that the channel will cascade to the outfall using a steepest hillslope descent. The special handling of a channel cell involves the conceptualization of the grid cell containing a channel. Figure 14 shows how the $\ln(a/\tan\beta)$ flow concepts are handled for the special flagged cells. It is assumed that the slope angle $\tan\beta$ is the average of all the upslope angles and that the contour length is equal to the sum of both sides of the channel. It is also assumed that the channel runs directly across the grid cell with a length equal to the grid size. This is a simple conceptualization and is open to modification.

The effect of introducing a channel into the algorithm causes the very high values of the index along the

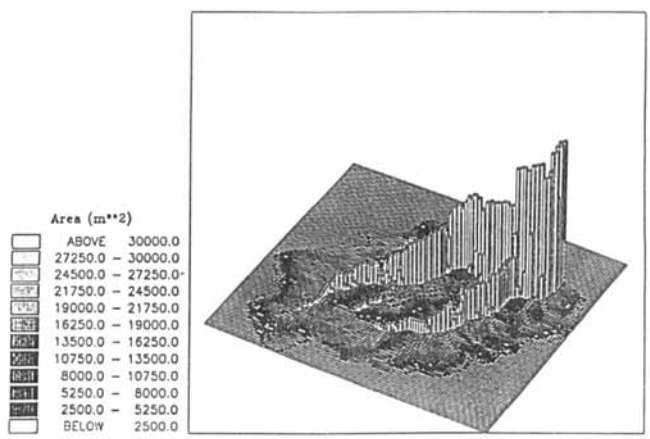

Figure 13. Flow accumulation anomaly of the existing theory that does not include the effect of channels

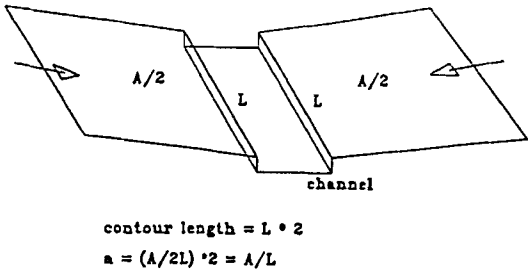

Figure 14. Possible conceptualization of a 'hillslope cell containing a channel', where A is upslope area and L is the length of the channel

channel, as contained in the tail end of the distribution function, to disappear. Figure 15 shows the ln(a/tanβ) distribution function for a range of CIT values as tested on the 50 m DTM. For the thresholds of 250 000, 40 000 and 22 500 m^2, the values in the tail-end of the distribution are progressively removed and shifted back into the heart of the distribution. This is in effect converting 'channel cells' back into 'hillslope cells containing a channel'. The 5000 m^2 threshold is discussed below.

When carrying out TOPMODEL simulations involving the use of a CIT, little change in the hydrographs was seen, but the pattern of the variable source areas changed dramatically. The problem was that if the CIT was set incorrectly, then unrealistic variable source area patterns were generated. Figure 16 shows this problem. In Figure 16A, the CIT was set too high and the problem of bias in the a term continued — that is, flow accumulation continued up to the channel before disappearing into the channel (as in Figure 13). This leads to the prediction of long linear variable source areas above the channel head, which is logically inconsistent with the assumptions of the algorithm. However, if the field evidence suggested the existence of such features, then this is one method by which they can be achieved. The field hydrologist may even be able to suggest which CIT to use. Figure 16B illustrates the converse of this case where no visible flow accumulation can be distinguished. If the CIT is too low, then there is little chance for flow accumulation to occur, and in essence too many 'hillslope cells' are being turned into 'hillslope cells containing a channel'. This leaves the question as to whether there is an optimum threshold for channel initiation?

Where is the river?

In an attempt to gain a logically consistent flow accumulation map, detailed analysis of the interaction of CIT values on the distribution function was carried out. Firstly, using the 50 m DTM a successively lower CIT was introduced (as is seen in Figure 15). The former 'channel cells' are turned back into 'hillslope cells

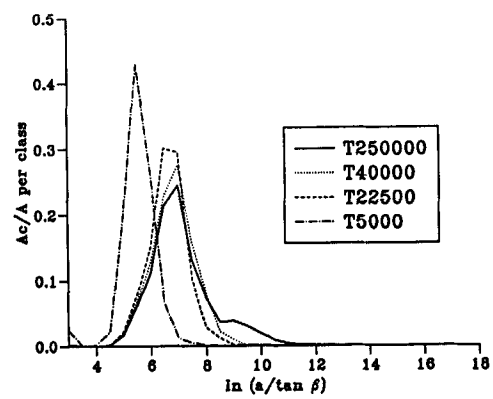

Figure 15. Change in the ln(a/tanβ) distribution function by introducing a successively lower CIT value

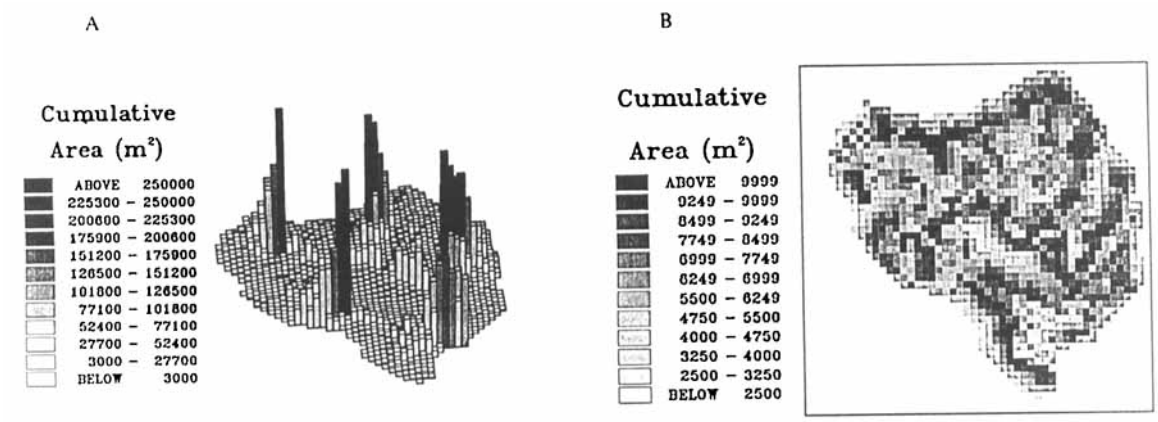

Figure 16. Artefact features of choosing a poor CIT value. (A) Continued flow along channels as in Figure 13. (B) In plan view, little visible flow accumulation is seen due to the low threshold

containing a channel' and now have a lower index value. This leads to a small increase in the peak of the distribution as the CIT decreases. However, there come a point when the shape of the distribution changes rapidly, exhibiting a rapid increase in the (Ac/A) value in the peak and a shift of the position of the peak to a lower value (see Figure 15). This occurs rapidly despite only a small change in the CIT value. The point at which this rapid change occurs is interpreted as the optimum value for a channel ending. Once reached, the channel is rapidly extending onto the hillslope portion of the DTM. Hence this causes a large shift in the distribution function form. This optimum value is thus taken for the initiation threshold for the channels. We are not trying to suggest that this CIT value is the 'true' position of the channels as measured in the field. It is only being proposed here that this value is the optimum position of the channel for this particular DTM resolution and is consistent with the aims of TOPMODEL and the assumptions of the analyses. By using this optimum CIT value, long thin variable source areas are avoided (i.e. removing any bias induced by 'channel cells'). Also, this value stops too many hillslope cells being turned into 'hillslope cells containing a channel' (i.e. creating a situation more akin to the single flow direction algorithm).

By such an analysis it should be possible to define an optimum CIT value. Figure 17 shows how three of the distribution function shape parameters change as progressively lower CIT values are introduced. The first is the position of the peak of the distribution on the $\ln(a/\tan\beta)$ axis; this is seen to have the sharpest response in behaviour. The second is the value of Ac/A at the peak of the distribution. After the small increase in the value of Ac/A, due to 'channel' cells being turned into 'hillslope cells containing a channel', there is a rapid increase in the Ac/A value. Finally, as the $\ln(a/\tan\beta)$ index is being calculated, a map of the channel network is produced and the number of flagged cells can be counted. Hence a third graph shows the number of channel cells within the DTM for a particular CIT threshold. Again there is sharp rise in the number of flagged 'cells containing a channel' close to the optimum CIT value. It is not necessary to extract an exact CIT value for analysis, but a value close to the maximum change in the distribution shape would minimize artefact variable source area features. An optimum CIT value of 22 500 m^2 was used to define the channel network or riparian for the 50 m DTM. Figure 18 is a map of the flagged cells that contain channels and their associated riparian areas. From this map it should be possible to estimate the channel and riparian area — that is, the area of likely rapid runoff. Figure 18 is now a map showing cells likely to produce a rapid runoff response to rainfall and, as such, has been removed from the $\ln(a/\tan\beta)$ map and should be treated separately.

As already stated, the optimum CIT for the 50 m DTM was estimated only for that particular DTM. Hence to study the effect of using a smaller grid size on the optimum CIT, the procedure was repeated with the 5 m DTM. Figure 19 shows these results. The same behavioural pattern was derived but now the CIT value is 2000 m^2. This is a factor of 10 smaller than that of the 50 m DTM. The conclusion is the CIT must be derived for each pixel resolution. It may also be necessary to repeat the analysis for

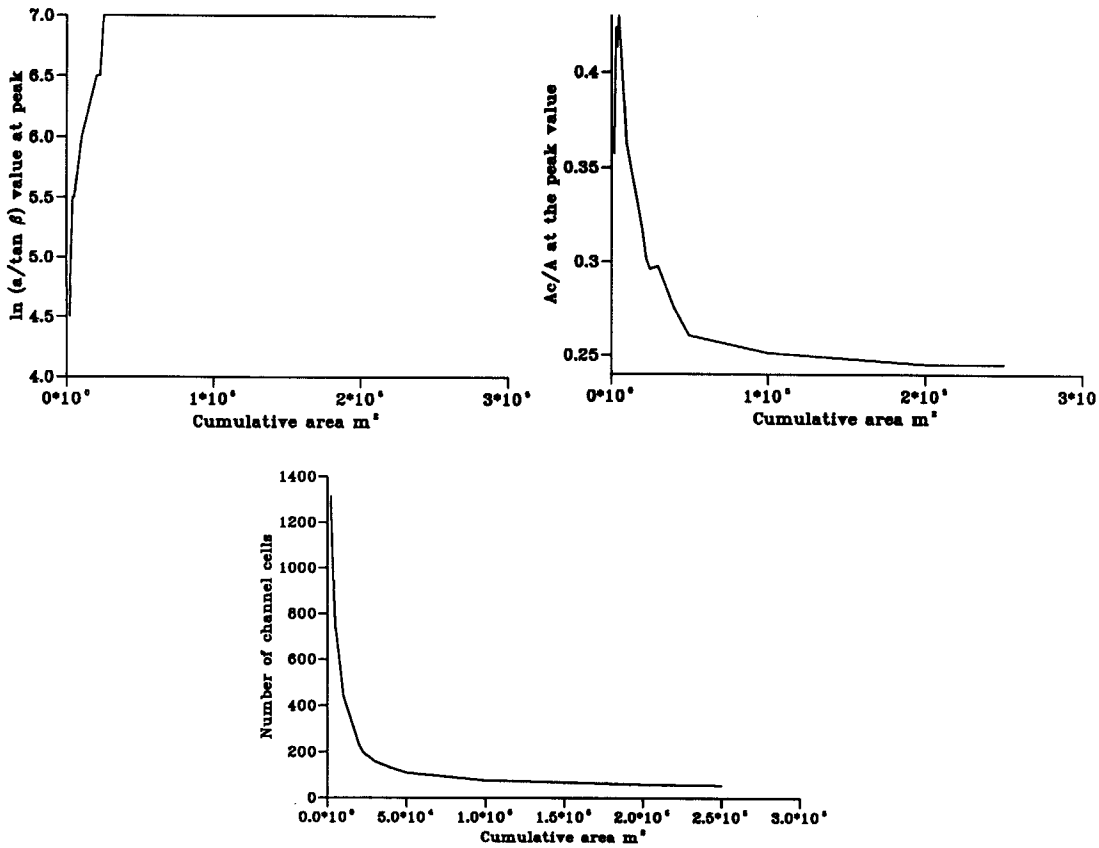

Figure 17. Changes in ln(a/tanβ) distribution function form by changing the CIT value. The optimum CIT for 50 m grid cells can be chosen in the zone just before the ln(a/tanβ) distribution changes rapidly

each individual catchment. Any attempt to use the 50 m CIT of 22 500 m^2 on the 5 m DTM results in no affects the distribution function shape. If the CIT is too high for the 5 m DTM, the original cumulative area bias will persist. Smaller grid cells and a smaller CIT both infer a longer channel network with a higher drainage density and hence a larger riparian area, which has implications for runoff production.

The new typical ln(a/tanβ) pattern for the 50 m DTM is shown in Figure 20. This should be compared

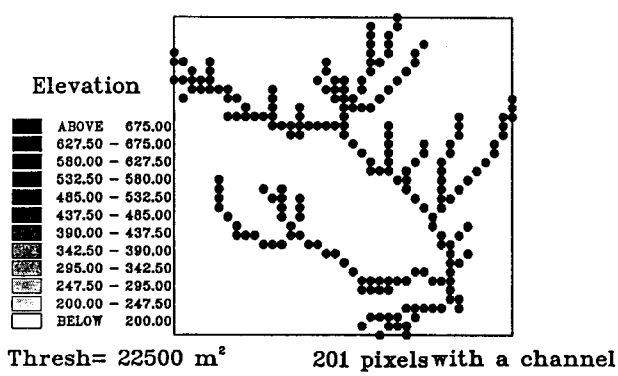

Figure 18. Corresponding channel network determined for the optimum CIT of Figure 17. This is an indication of the riparian area needed to be included in the model calculations

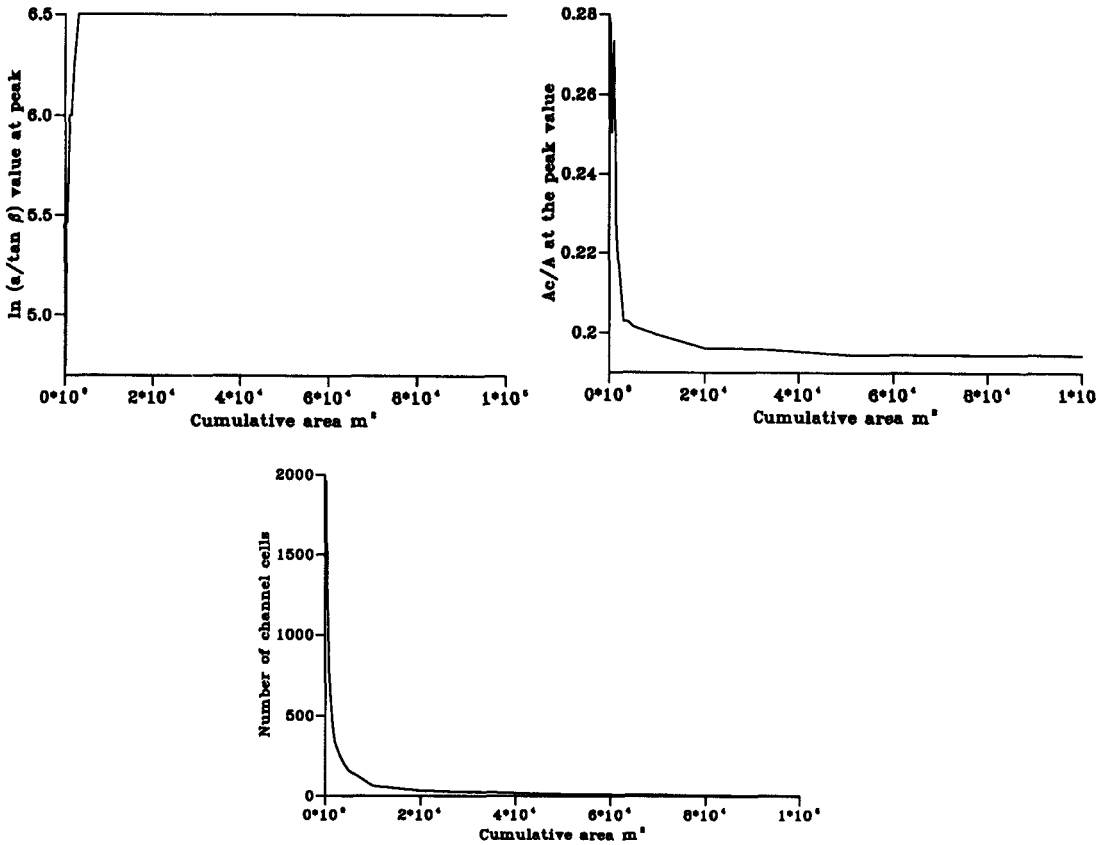

Figure 19. Optimum CIT choice for the 5 m DTM of Figure 6A

with Figure 5. It can be seen that the dark valley bottom feature has all but gone, and that all variation is now taking place on the hillslope. It must be remembered that this map will still have a riparian area, but that the riparian area is no longer exhibited on the index map. Some people may suggest that this pattern is not as communicative of catchment form as the original routine, and visually it is not as intuitively pleasing. However, this is more likely to raise the question as to why the original pattern is so popular despite the assumptions of the algorithm being unrealistic. It is probably true that this pattern is not as informative as the original map as it can be seen there are too few cells between the catchment divide and the river

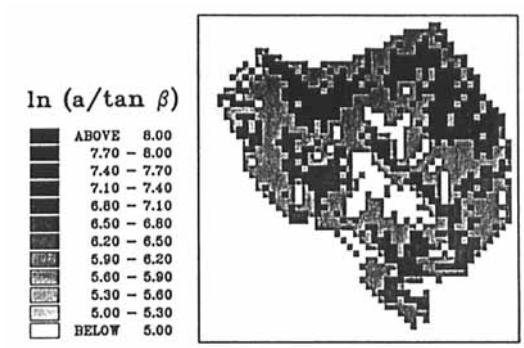

Figure 20. New index map of the control DTM (Figure 5), including the optimum CIT. This shows some catchment structure but the valley floor feature has gone

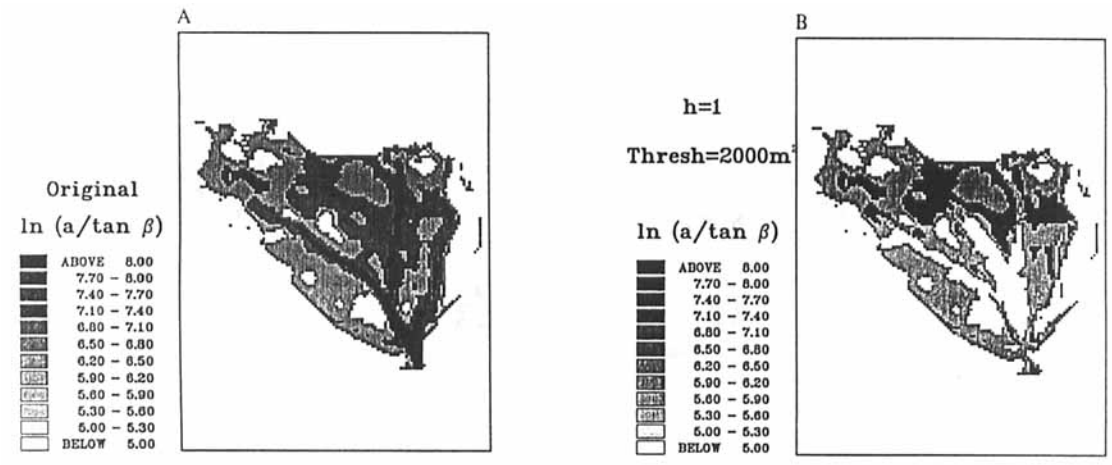

Figure 21. Comparison of the original ln(a/tanβ) pattern for Figure 6A and the new pattern including the effect of channels

cells to create enough variation in the index. When there are many pixels in the original pattern, then the pattern looks correct. This point was raised earlier as regards Figure 6A and 6D, where the 50 m DTM for the headwater catchment showed only the overall gradient of the hillslope and most of the variability had been smoothed out. It was also stated that the 5 m DTM for the headwater had an intuitively pleasing pattern. It may be concluded from this study that, for the purposes of internal validation of TOPMODEL, 50 m is too large or unrepresentative, and that a smaller grid scale DTM should be used. Perhaps DTMs of the order of 10 m or smaller are needed to capture the variability in topographic form for hillslopes of this scale.

Figure 20, as stated, does not show great variability in the index when the optimum CIT is used. Once again the same test was carried out on the 5 m headwater DTM in Figure 21. Figure 21B shows the disappearance of the large dark area associated with the channel areas compared with the original of Figure 21A. However, much of the hillslope variability can be seen. As stated above, the derived riparian area is not shown on Figure 6B and must be treated separately.

A COMBINED CIT AND $(\tan\beta)^h$ INDEX

A final suggestion is now introduced that is a combination of the CIT and power h variables mentioned above. This concept assumes that the permanent channel can be defined, but the power factor used for flow apportioning is also related to the accumulated upslope area. This idea was inspired by hydrological fieldwork in Alaska (Ostendorf, personal communication.) It was suggested that a routine was written that commenced with a full multiple flow direction algorithm near the catchment divide (i.e. that h was equal to unity). However, as the flow approached the permanent channel the flow should become progressively straighter. In essence, as the amount of upslope area increased, then the flow became more unidirectional. As the concept of a CIT has been introduced it is possible to model this downslope feedback effect using the following power term

$$d_i = cld \tan\beta^f$$

where

$$f = [A/thresh) + 1]^h$$

A = current upslope area; $thresh$ = the current CIT value chosen by the user; h = the adjustable power term; and cld = is the same as the original formulation.

The value of $A/thresh$ will fluctuate between 0 and 1 hence, the value 1 was added. At low $A/thresh$ the resulting power will be close to 1, thus giving the multiple flow direction algorithm. As the cells approach

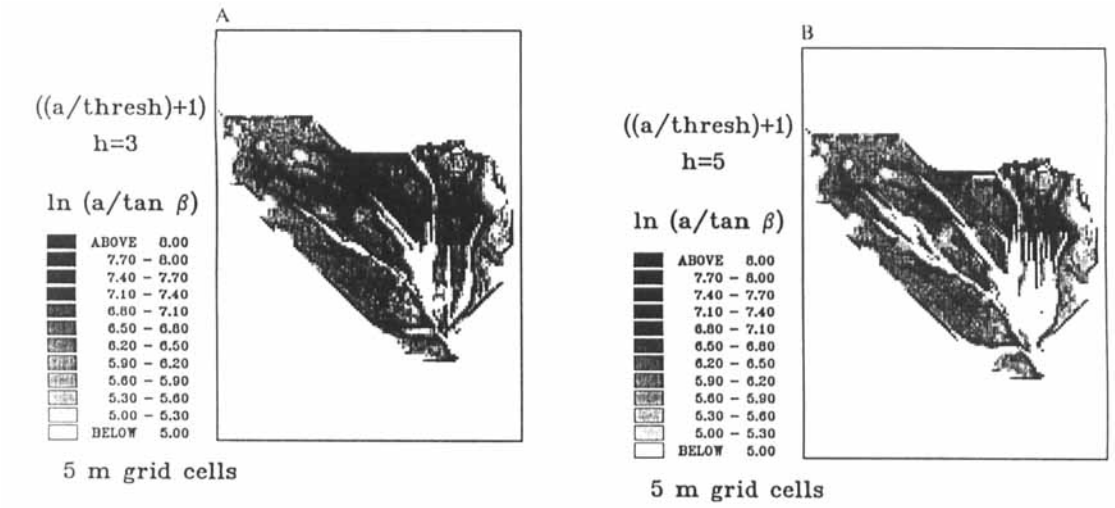

Figure 22. Two examples of how the $\ln(a/\tan\beta)$ pattern can be manipulated by using the 'feedback' algorithm index for the 5 m DTM. The CIT value is the optimum value in both (A) and (B)

the specified CIT value a straighter flow direction will occur. The degree of straightening is dependent on the h value. Higher values of h tend to give a stronger contrast in the index map. This is equivalent to a faster change from multiple to single flow direction accumulation.

The effect on the 50 m DTM was very limited and no significant change in the index pattern occurs. This is again due to the lack of cells between the divide and the specified channel. An example is shown in Figure 22 for the 5 m DTM. The effect on the 5 m grid cells is much greater due to the increase in the number of cells between divide and the channel. Figure 22A shows the index map when $h = 3$ and the CIT is at the optimum value of 2000 m^2. This is different to the patterns suggested in Figures 12B and 21B, where the power of h is used on every grid cell. The likely variable source areas are now seen above the channel heads and near the interfluve. This pattern is changed by the increase of h, as shown in Figure 22B. The size of the variable source areas above the channel heads has decreased in size and some linear features likely to saturate are seen close to the specified channel.

A NEW TOPMODEL FRAMEWORK

It is hoped that the above discussion will help TOPMODEL users to appreciate some conclusions arising from spatial analysis

1. Optimized parameter sets change with grid size. Calibrated TOPMODEL parameter sets, h values and CITs are not transferable between grid resolutions
2. There is no one solution for calculating the $\ln(a/\tan\beta)$ index. In most catchment studies workers will probably find that they have to optimize the pattern of the index to fit their own field observations

The user now has three options and two calibration parameters within the index to manipulate the final index pattern

1. The h parameter of Holmgren (1994), similar to the p parameter of Freeman (1991)
2. The CIT, which may or may not be set to an optimum value, depending on the observations of the field hydrologist
3. Combination of the above two to create a 'feedback' version that can convert from fully multiple flow direction on the upper slopes into single flow direction before entering the permanent channel

There are two fundamental changes to the $\ln(a/\tan\beta)$ function due to the introduction of an optimum CIT

1. High values of the index, typically 12 plus, have now disappeared. It is very common in TOPMODEL applications to run the model with a range of 4 to 20, with an increment step of around 0·5. It is probably better with the new shortened distribution to use a range of 4 to 12 with an increment of 0·25 (or even smaller). The fact that the high values have disappeared does not mean that the modelled variable source area will get smaller. If the model is reoptimized then the calibration parameters may readjust themselves to give the same proportion of quick flow response, i.e. there may be the same percentage of saturated area as in the original framework. However, the location of the variable source areas will now be different. The dominance of channel cells towards the outfall of the catchment will have gone and more runoff will be generated around the heads of channels and upstream generally
2. The feature approximating to a riparian area in the original analysis is now removed. Runoff production from the river cells (albeit river cells 50 * 50 m wide) was always very quick and intuitively acceptable for fast surface or subsurface responses. Hydrographs commonly show a very rapid response to storms due to riparian areas despite long interstorm periods. To maintain this quick runoff effect it is recommended that a direct proportional area multiplier is used to create instantaneous runoff from the model. It may be possible to fix this parameter from observations or hydrograph analysis.

All the above analysis has tended to point to the suggestion that smaller DTM resolutions may be needed for internal validation of the model. However, the simpler goal of predicting hydrographs can be achieved by using 50 m grids. In many circumstances it may not be possible to create a large DTM database with fine resolution cells because

1. Fine grid scale DTMs will not be available to most users. Most national databases will have 30–50 m DTM.
2. Any reduction in grid size in even a moderately small catchment causes a huge increase in data.
3. The conversion or creation of fine grid scale DTMs for large basins may be subject to greater interpolation errors.
4. More pixels will mean more processing time.

So, what compromise can be achieved to satisfy our goals of hydrograph prediction with minimum effort and validation of the model processes using internal state data? The following ideas are suggested.

If hydrographs only are required, then coarse DTMs using any of the above algorithms will suffice. Any inaccuracy in the distribution function form will be compensated by the TOPMODEL calibration parameters. However, the spatial predictions of these models should not be used for detailed proof of internal processes. These coarse DTMs will only communicate the overall macroscale operation of the catchment dynamics. There may be some scope to use remotely sensed data or vegetation indices for validation at these scales, if the validation data have the same resolution as the DTM.

If internal state data are to be used, then a fine grid scale DTM is required. If the distribution functions of smaller grid resolutions are a better representation of catchment variability, then they should more accurately model flow response. However, it is only feasible to have DTMs with a high enough resolution and trustworthy accuracy for small areas. Also required is that a flow gauge is placed in each subcatchment to be modelled so that effective parameters can be calibrated. It is recommended here that nested DTM data sets be used. A 50 m DTM can be produced for the whole basin or downloaded from a national GIS. This can be used to model landscape flux and show the macroscale operation of the basin. Nested DTMs with fine scale resolution data should then be used to validate the internal data. For the example shown in this paper, a small 5 m DTM was produced. However, this is a steep-sided convergent catchment and the predicted fluxes are typical of this area. It would be necessary to choose one or more typical representative subareas (to allow for divergent slopes or parallel slopes). It is then relatively easy to classify the remainder of the catchment as being closest to one of the subsampled representative DTMs. The percentage of the area within the basin of each type (convergent, divergent and parallel) can then be used to create the final distribution function for the whole basin. The internal state measurements should then be concentrated in each of the typical subareas. Using the optimized values of TOPMODEL and the local index patterns of the subareas the internal validation procedure can continue. It is likely that the internal validation will not be easy as local heterogeneity is at its

highest and some calibration of the index pattern will be needed. This next phase of research will be interesting and most revealing. It is desirable that the field measurements become larger than the point scale. Perhaps techniques such as ground penetrating radar can help in the visualization of 'local' phenomena such as the pattern of water-table movement over larger areas.

A brief test was made to show that the above recommendations are plausible. A three month period of hourly rain, flow and evaporation data were taken from the Wye catchment and the model produced by Quinn and Beven (1993) was used to test the accuracy of changing the TOPMODEL DTA assumptions. The following runs were made and the accuracy of the models was described by a simple Nash efficiency, E, calculation

1. The control run is from Quinn and Beven (1993) for three months of data in a rainy period. The 50 m DTM of Figure 1 was used to create the distribution function. The model gave $E = 90\%$ after optimization
2. Using the optimized parameters of (1) and the distribution function derived from the 5 m DTM of Figure 6A for the same period, $E = 86\%$. This is largely due to the fact that the temporal function in TOPMODEL (Figure 2) is equally important for predicting good hydrographs. This temporal function is hardly altered by modification of the spatial function. Also, the overall shape of the $\ln(a/\tan\beta)$ distribution functions as shown in Figure 8 is not very different
3. Using (2) an optimization run was made for the same period. The final model gave $E = 90\%$ — that is, the optimization process had returned the model to its former accuracy, although 4% is a very small amount in modelling terms. As suggested, the optimization parameters have altered the final model response
4. The use of the 50 m DTM using an optimum CIT but altering the range of the index from 3 to 12 and using a 0·25 step. Using the same parameters as in run (1), $E = 89\%$

The conclusion of the above study is that, if the overall spatial distribution functions have roughly the same shape, then interchangebility is possible while maintaining good hydrograph prediction. This as stated is largely due to the fact that the temporal function is the major factor controlling the fit of the hydrographs and affects the Nash E in a strong way. Any accuracy lost in the spatial function can be minimized by re-optimizing the parameters for the new situation. This conclusion is supported by the work of Bruneau et al. (in press), where both the model grid size and the model time step were varied. They show for a model grid size within a sensible range of 5–100 m that the model efficiency is not significantly changed when the model is re-optimized. They also show that for the same change in the $\ln(a/\tan\beta)$ distribution as seen in this study — that is, for a smaller grid cell size — the whole of the distribution would be shifted to a lower $\ln(a/\tan\beta)$ value. Bruneau *et al.* (in press) go on to show that during optimization the T_0 parameter would change to offset the shift in the position of the overall distribution function. This shift typically shows a increase in T_0 with an increase in grid size.

It is suggested that the above recommendations are followed for modelling hydrographs and performing internal process validation.

CONCLUSIONS

Two new concepts have been examined. Firstly, the manipulation of the flow from cell to cell can be altered by using the power $(\tan\beta)^h$ or the feedback version $(\tan\beta)^f$, where $f = [(A/thresh) + 1]^h$. Secondly, the role of the channel interaction with the index has been discussed to make flow accumulation more realistic. The concept of the CIT was introduced for defining 'hillslope cells containing a channel'. As the CIT can cause artefact patterns in the variable source areas, a test can be made to give an optimum CIT. It is not suggested that the optimum CIT is good prediction of the 'true' channel position. It is suggested that this is the optimum channel position given the current DTM resolution and the assumption of the TOPMODEL DTA.

The problems resulting from a change in grid size can be summarized in two sets of conclusions

1. Large pixels are unrepresentative of detailed catchment form but are still useful for macroscale interpretation of moisture flux and the prediction of hydrographs. Nested representative DTMs with fine resolution should be used to test internal state processes as 50 m data are too coarse for point field data to validate. The shape and size of a catchment may alter if large cells are used in small subcatchments. Finally, a large pixel resolution will give a bias towards large ln(a/tanβ) values.
2. All analysis should be made appropriate to a particular grid scale and parameters are not transferable between grid resolution. This includes the optimum CIT, the h power and the final TOPMODEL optimized parameter sets.

As future studies proceed, the arrival of new spatial data sets will test the DTA processes in detail. It will probably be necessary to alter the final index pattern by calibrating the index pattern to improve the simulation of variables observed in the field. This manipulation of the spatial function will not limit the model's capability to predict hydrographs.

In the absence of conclusive field data or field methodologies there is no one best method of creating topographic indices. The reader should regard this study as a definition of some of the problems and possibilities for model application.

ACKNOWLEDGEMENTS

Many thanks must be given to Peter Holmgren and to Bo Ostendorf for making us realize that our digital terrain analysis job was not complete by their useful comments and their bright ideas. Other thanks go to the Lancaster TOPMODEL group.

REFERENCES

Band, L. 1986. 'Topographic partition of watersheds with digital elevation models', *Wat. Resour. Res.*, **22,** 15–24.

Beven, K. J. 1986. 'Runoff production and flood frequency in catchments of order n: an alternative approach' in Gupta, V. K. and Rodriguez-Iturbe, I. (eds), *Scale Problems in Hydrology*. Reidel, Dordrecht. pp. 107–131.

Beven, K. J. 1987. 'Towards a new paradigm in hydrology. Water for the future: Hydrology in perspective', *IAHS Publ.*, **164,** 393–403.

Beven, K. J. 1989. 'Changing ideas in hydrology — the case of physically-based models', *J. Hydrol.*, **105,** 157–172.

Beven, K. J. and Kirkby, M. J. 1979. 'A physically-based variable contributing area model of basin hydrology', *Hydrol. Sci. Bull.*, **24,** 43–69.

Beven, K. J. and Moore, I. D. (Eds) 1993. *Terrain Analysis and Distributed Modelling in Hydrology*. Wiley, Chichester.

Beven, K. J., Kirkby, M. J., Schofield, N., and Tagg, A. F. 1984. 'Testing a physical flood forecasting model TOPMODEL for three U.K. catchments', *J. Hydrol.*, **69,** 119–143.

Bowles, D. S. and O'Connel, P. E. (Eds) 1991. *Recent Advances in the Modelling of Hydrologic Systems*. Kluwer Academic, Dordrecht.

Bruneau, P., Gascuel-Odoux, C., Robin, P., Merot, P., and Beven, K. J. 'The sensitivity to space and time resolution of a hydrological model using digital elevation data', *Hydrol. Process.*, in press.

Chairat, S. and Delleur, J. W. 1993. 'Effects of the topographic index distribution on the predicted runoff using GRASS', *American Water Resources Association. Symposium on Geographic Information Systems in Water Resources, Mobile Alabama, USA, March 1993.*

Dunne, T. and Black, R. D. 1970. 'Partial area contributions to storm runoff in a small New England watershed', *Wat. Resour. Res.*, **6,** 1296–1311.

Famiglietti, J. S. and Wood, E. F. 1991. 'Evapotranspiration and runoff from large land surfaces heterogeneity in climate models' in Wood, E. F. (Ed.), *Land Surface–Atmosperic Interactions for Climate Modelling*. Kluwer, Dordrecht.

Freeman, T. G. 1991. 'Calculating catchment area with divergent flow based on a regular grid', *Comput. Geosci.*, **17,** 413–422.

Hewlett, J. D. and Hibbert, X. X. 1963. 'Moisture and energy conditions within a sloping soil mass during drainage', *J. Geophys. Res.*, **68,** 1081–1087.

Hewlett, J. D. and Troendle, C. A. 1975. 'Non-point and diffused water sources: a variable source area problem' in *Proceedings of Symposium on Watershed Management*. American Society of Civil Engineers, New York. pp. 21–46.

Holmgren, P. 'Multiple flow direction algorithms for runoff modelling in grid-based elevation models: an empiric evaluation', *Hydrol. Process.*, **8,** 327–334.

Hornberger, G. M., Beven, K. J., Cosby, B. J., and Sappington, D. E. 1985. 'Shenandoah watershed: calibration of a topography-based, variable contributing area hydrological model to a small forested catchment', *Wat. Resourc. Res.*, **21,** 1841–1850.

Moore, I. D., Mackay, S. M., Wallbrink, G. J., Burch, G. J., and O'Loughlin, E. M. 1986. 'Hydrologic characteristics and modelling of a small forested catchment in Southeastern New South Wales. Prelogging condition', *J. Hydrol.*, **83,** 307–335.

Morris, D. M. and Heerdegen, R. G. 1988. 'Automatically derived catchment boundaries and channel networks and their hydrological applications', *Geomorphology*, **1,** 131–141.

Nathon, R. J. and McMahon, T. A. 1990. 'Evaluation of automated techniques for baseflow and recession analyses', *Wat. Resour. Res.*, **26,** 1465–1473.

O'Callaghan, J. F. and Mark, D. M. 1984. 'The extraction of drainage networks from digital elevation data', *Comput. Vis. Graphics Image Process.*, **28,** 323–344.

O'Loughlin, E. M. 1981. 'Saturation regions in catchments and their relations to soil and topographic properties', *J. Hydrol.*, **53,** 229–246.

O'Loughlin, E. M. 1986. 'Predictions of surface saturation zones in natural catchments by topographic analysis', *Wat. Resour. Res.*, **22,** 794–804.

Quinn, P. F. and Beven, K. J. 1993. 'Spatial and temporal predictions of soil moisture dynamics, runoff, variable source areas and evapotranspiration for Plynlimon, Mid-Wales', *Hydrol. Process.*, **7,** 425–448.

Quinn, P. F., Beven, K. J., Chevallier, P., and Planchon, O. 1991. 'The prediction of hillslope flowpaths for distributed modelling using digital terrain models', *Hydrol. Process.*, **5,** 59–80.

Robson, A., Beven, K. J., and Neal, C. 1992. 'Towards identifying sources of subsurface flow: a comparison of components identified by a physical based runoff model and those determined by chemical mixing techniques', *Hydrol. Process.*, **6,** 199–215.

Rodriguez-Iturbe, I. and Valdes, J. B. 1979. 'The geomorphic structure of hydrologic response', *Wat. Resour. Res.*, **15,** 1409–1420.

Sklash, M. G. and Farvolden, R. N. 1979. 'The role of groundwater in storm runoff', *J. Hydrol.*, **43,** 45–65.

Strahler, A. N. 1957. 'Quantitative analysis of watershed geomorphology', *Trans. Am. Geophys. Union*, **38,** 913–920.

Tarboton, D. G., Bras, R. L., and Rodriguez-Iturbe, I. 1991. 'On the extraction of channel networks from digital elevation data', *Hydrol. Process.*, **5,** 81–100.

Wood, E. F., Sivapalan, M., Beven, E. F., and Band, L. E. 1988. 'Effects of spatial variability and scale with implications to hydrologic modelling', *J. Hydrol.*, **102,** 29–47.